JOURNAL OF MATERIALS SCIENCE **36** (2001) 3629–3635

Structural aspects of α/β transformation in hot deformed CuZn-39Pb3 alloy

LUDWIK BLAZ, ZDZISLAW KONIOR, TERESA MAJDA
Academy of Mining and Metallurgy, Department of Structure and Mechanics of Solids, Al.Mickiewicza 30, 30-059 Cracow, Poland

Hot compression tests were performed on commercial CuZn39Pb3 alloy deformed at strain rate of 0.0007 s^{-1} and 0.02 s^{-1} within temperature range of 923 K–1023 K. Flow stress vs. deformation temperature and strain rate dependence was found to follow the relation: $\dot{\varepsilon} = 1.23 \cdot \sigma^{3.79} \exp(-212/RT)$. Both dynamic recovery and dynamic recrystallization have operated in the presence of fine lead particles being responsible for effective flow stress reduction with increasing deformation temperature. Transformation of α- to β phase above the temperature approx. 1000 K and the following fast cooling of hot deformed samples produced fine, plate-like structure of α-grains, within retained β-matrix. Moreover, coherent fine Fe-particles were observed within α-grains being not detected at any area of β-matrix. The last effect was supposed to result from lower solubility of iron in α-phase than that for β-phase.

1. Introduction

Hot deformation procedures are commonly used in industrial practice in order to reduce the final cost of products. The load reduction with temperature and an increase of material ductility may efficiently increase the total output and save the energy for shaping of the material. However, except of the product cost, the customers are also interested in the structure and mechanical properties of the material. Because of that, it is important to know how deformation conditions affect the total material properties and how to control the deformation conditions in order to produce the desired structure of the material. Leaded brass is widely used in industrial practice mainly due to pretty good machinability, water resistance and good mechanical properties. Addition of lead during casting results in dispersed distribution of lead particles in the matrix that effectively reduces grain coarsening during annealing and increases both the hardness and the strength of the material. However, because of very low ductility at room temperature, the material must be shaped at high deformation temperatures in order to avoid brittle cracking and fracture of the product. Both low strain rate and high temperature of deformation promote the structural softening processes, which reduce strain hardening and cavity growth during hot deformation of the alloy. For metals and single phase alloys of low stacking fault energy (SFE), dynamic recovery and dynamic recrystallization are responsible for the flow stress reduction during high temperature deformation [1]. However, alloying elements and impurities, which are practically always present in industrial-type alloys, may effectively retard the softening processes and result in limited ductility of the hot deformed material. The most effective retardation of the dynamic softening processes may result from grain boundary pinning by fine particles [2]. In the presence of dispersed second phase particles, dynamic recrystallization can be completely retarded and dynamic recovery becomes the sole softening process.

During hot deformation of commercial α–brasses above the *solvus* temperature, $\alpha \rightarrow \beta$ phase transformation was observed. At low strain rates, the nucleation and growth of β-grains at pre-existing grain boundaries and highly recovered substructure, effectively reduced dynamic recrystallization. In result, any detectable flow stress peaks preceded the steady state flow range. Dynamic recovery was found to operate very effectively at high deformation temperatures and highly recovered substructure was created within the matrix. Overlapping of β-grains growth and structural dynamic restoration processes affected the flow stress value as well as the final properties of a hot deformed material [3, 4].

Dynamic precipitation during hot deformation of Cu-Ti and Cu-Ni-Cr-Si-Mg alloy was observed for solution treated samples deformed below the *solvus* temperature [5–8]. Continuous precipitation of metastable and fine particles at the initial stage of aging resulted in intense strain/aging hardening of the hot deformed material. At larger strains and high enough temperature, an interaction of shear banding and continuous precipitation process resulted in the particles dynamic coarsening within shear bands. In result, the flow stress value was effectively reduced during hot deformation.

Contrary to the discontinuous precipitation effect, foregoing continuous nucleation of metastable fine particles at the early stage of aging was found to promote localized flow without any detectable effect of localized flow on particles nucleation and growth. It should be stressed that the phase transformation $\alpha \Leftrightarrow \beta$ at Cu-Zn-Pb alloy does not follow similar sequences to

those described for Cu-Ti or Cu-Ni-Cr-Si-Mg alloy. At hot deformed Cu-Zn-Pb alloy, both stable lead particles and $\alpha \rightarrow \beta$ transformation should affect the structural dynamic processes. Having in mind the specific differences for the phase transformation process at the mentioned alloys, it was interesting to compare the structural and the mechanical effects of strain/transformation interaction during hot deformation of commercial CuZn39Pb3 alloy.

2. Experimental

Experiments were performed on as received industrial-type leaded brass (CuZn39Pb3). Chemical composition of the alloy was given in Table I. Cylindrical samples, 9 mm in diameter and 12 mm in height, were cut from hot extruded and cold drawn rod. The edges, 0.2 mm in size, were machined at both sides of the sample in order to maintain the lubricant during the compression test. Then, the samples were annealed at 1023 K/60 min. and air-cooled.

Hot compression tests were performed on MTS testing machine equipped with high temperature furnace and a fast cooling system. Samples were deformed at the strain rate of 0.0007 s^{-1} and 0.02 s^{-1} within the deformation temperature range 723 K–1093 K and quenched in water within ~1 s after deformation had stopped. Flaked graphite was used as a lubricant in order to reduce the friction of the sample against the anvils. Details of the equipment were given elsewhere [9].

Hot deformed samples were cut along the compression direction and prepared for optical microscopy observations. Slices for transmission electron microscopy observations were cut along compression axis from the central part of the samples. Thin foils were prepared using the ion beam thinning method on GATAN 691 PIPS. TEM observations were performed on 200 kV JEOL 2010 ARP electron microscope equipped with a scanning transmission electron microscopy device (STEM) and OXFORD LINK-PENTAFET X-ray analysis system.

3. Results and discussion

A typical set of flow stress curves for hot deformed Cu-Zn-Pb alloy was shown in Fig. 1. Logarithmic scale for true stress axis was used in order to mark the flow stress oscillations at high deformation temperatures. Assuming that a steady state flow stress range was reached within the experimental deformation range, the following flow stress-temperature-stress-strain rate relation can be used [1]:

$$\dot{\varepsilon} = A \cdot \sigma^n \cdot \exp\left(-\frac{Q}{RT}\right)$$

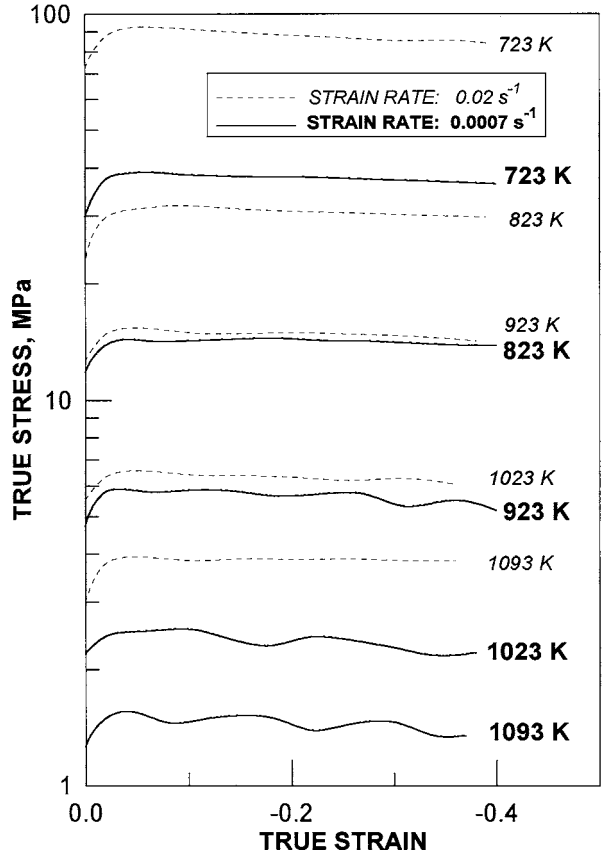

Figure 1 True stress–true strain curves received for CuZn39Pb3 alloy deformed at strain rates of 0.0007 s^{-1} (full lines) and 0.02 s^{-1} (dashed lines). Deformation temperature was marked in the figure.

where: A, n, = constants, Q = activation energy, R = gas constant, $\dot{\varepsilon}$ = true strain rate, T = temperature.

Mathematical constants (A, n) and activation energy for the hot deformation, $Q = 212$ kJ/mol, were calculated by the statistical least square method. In result, the formula (1) could be written in the form:

$$\dot{\varepsilon} = 1.23 \cdot 10^6 \cdot \sigma^{3.79} \exp(-212000/\mathrm{RT})$$

Zener-Hollomon parameter (Z) is commonly used to convert two deformation parameters, i.e. $\dot{\varepsilon}$ and T, into one parameter, Z:

$$Z = \dot{\varepsilon} \cdot \exp(Q/RT).$$

Thus, the flow stress value could be related to Zener-Hollomon parameter as was shown in Fig. 2.

Structural observations were performed on hot deformed samples as well as on samples annealed at the given temperature for a period of time that was equal to the sample deformation time. Such approach to the structural analysis has allowed comparing the material structure affected by static or dynamic processes. Typical structure of samples annealed for 3 min (a) and

TABLE I Chemical composition of CuZn39Pb3 alloy

Element:	Cu	Zn	Pb	Fe	Sn	Mn	Ni	Si	Cd	Sb
wt. %	in balance	38.31	2.89	0.224	0.132	0.006	0.035	0.010	0.039	0.006

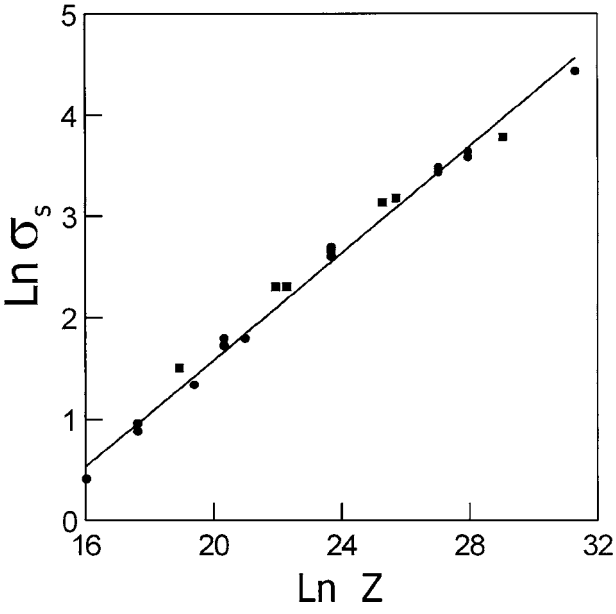

Figure 2 Flow stress vs. Zener-Hollomon parameter dependence for hot deformed CuZn39Pb3 alloy.

15 min at 1023 K (b) and a hot deformed one at 1023 K (c) was shown in Fig. 3. The time for sample heating and temperature stabilization before hot compression test was approx. 3 min. Thus, Fig. 3a represents the structure for the material at the beginning of deformation. The following deformation time was approx. 12 min. at the strain rate of 0.0007 s^{-1}. The structure of a hot deformed sample was displayed in Fig. 3c. For comparison purposes, the structure of the sample statically annealed for 15 min. at 1023 K was shown in Fig. 3b. The initial grain size of the material was approx. 3 μm and the volume of β-phase was less than 10%. In result of grain coarsening during the following 12 minutes of annealing, the grain size of approx. 10 μm in size was obtained and the β-grains practically disappeared. If instead of static aging, the hot deformation proceeded during 12 min. ($\varepsilon_t = 0.4$ at 0.0007 s^{-1}), the material structure was changed effectively due to both dynamic recrystallization and the following water quenching effect. The grains, coarsened due to dynamic recrystallization, were then refined during cooling because of $\beta \rightarrow \alpha$ phase transformation.

Colonies of elongated grains, 1–2 μm thick, were created at pre-existing grain boundaries and within grain interiors. Typical structure of a sample deformed at 1023 K and water quenched was shown in Fig. 4a.

Structure of the material annealed at 873 K–973 K or hot deformed in the same temperature range, was similar to those displayed in Fig. 3a and b. Grain refining due to $\beta \rightarrow \alpha$ transformation was negligible. However, for samples annealed and deformed at higher temperatures (above $\sim$1023 K) remarkable grain coarsening was observed. Fast cooling of coarse-grained material resulted in needle-like structure growth and grain refining due to phase transformation was observed.

The analysis of structural components using the selective etching method and optical microscopy was not successful enough to distinguish β- and α-grains within fine grained structure (grain size $\leq$5 μm). In order to determine α and β phases, transmission electron microscopy analysis had to be performed. Diffraction patterns from the neighboring fine grains allowed detection of α and β-grains within the sample structure. An example of mixed structure of α and β-grains that were grown within the interior of a pre-existing β-grain was shown in Fig. 4. Both highly recovered subgrains within α-grains (Fig. 4a) and fine α or β–grains (Fig. 4b) were very similar in shape and their size. Thus, they could not be distinguished by the use of optical microscopy techniques.

Both fine grained α/β-structure and highly recovered substructure within hot deformed grains, were

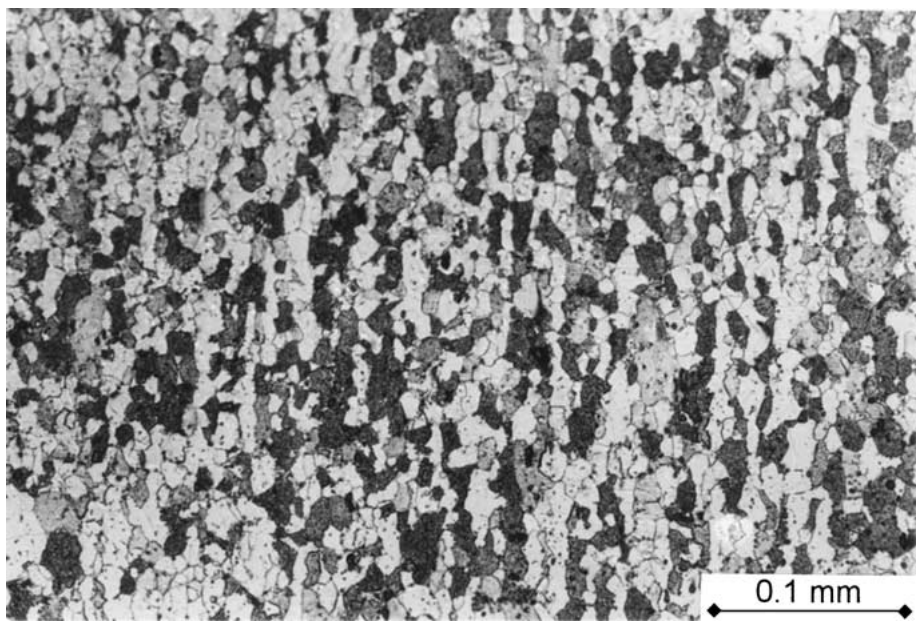

(a)

Figure 3 Structure of CuZn39Pb3 alloy: (a) annealed 3 min. at 1023 K; (b) annealed 15 min. at 1023 K; (c) hot deformed at strain rate of 0.0007 s^{-1} and temperature of 1023 K (deformation time: approx. 12 min.) *(Continued)*.

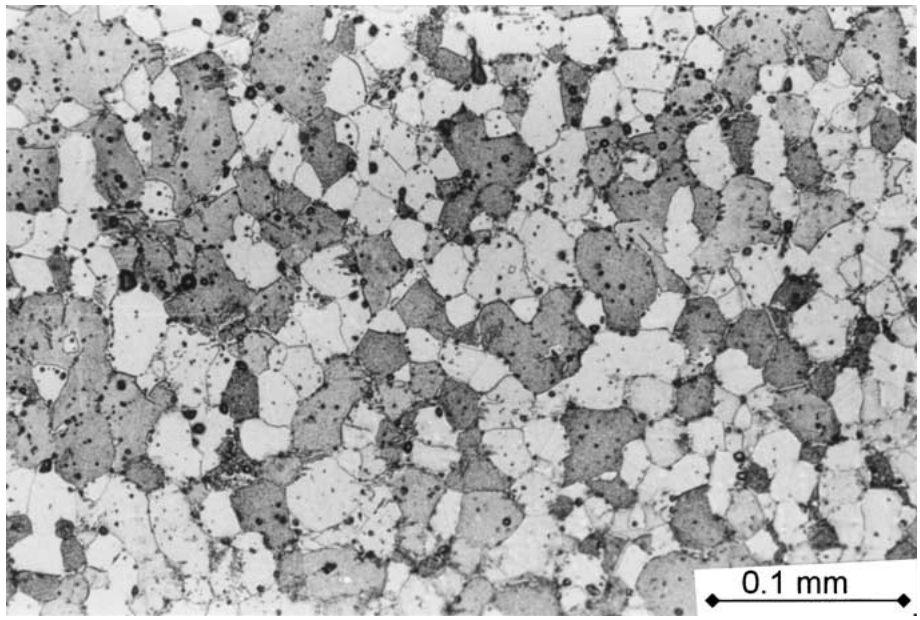

(b)

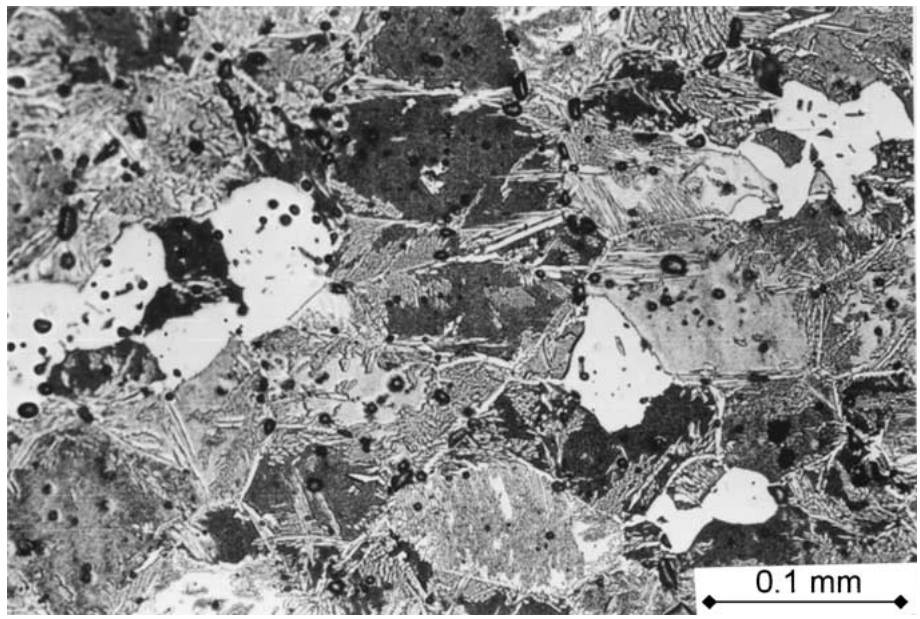

(c)

Figure 3 (Continued).

responsible for the material hardness increase for samples deformed at high temperature range (Fig. 6). Within the temperature range of 723 K–973 K, the strain hardening of hot deformed material was reduced with temperature. At higher deformation temperatures $\alpha \rightarrow \beta$ phase transformation and effective grain coarsening were observed. In result of fast cooling after hot deformation, coarsened β-grains were transformed into fine needle-like α/β grains. Both highly recovered substructure produced during hot deformation and grain refining after quenching were responsible for increased hardening of the material deformed above $\sim$1000 K.

It is worth mentioning that industrial Cu-Zn-Pb alloys contain some impurities and an alloying addition of specific elements. In particular, a small addition of iron and manganese is usually used in order to increase the mechanical properties of the alloy. In practice, Fe-Mn-rich particles are hardly soluble in the copper matrix. TEM observations performed on samples deformed within β-range (above 1000 K), revealed coherent Fe-particles within some grains or subgrains (Fig. 5). Energy disperse spectrum taken from the particle and the neighboring Cu-matrix, was displayed in Fig. 5b. Because of a very small diameter of the precipitates, quantitative analysis of the particle was not successful. However, high intensity of Fe-peaks has led to the conclusion about the dominating Fe-component of the particle. Basing upon the diffraction pattern analysis, it was also found that Fe-particles nucleated within α-grains and α-subgrains while the neighboring β-grains were free of precipitates. The effect of the

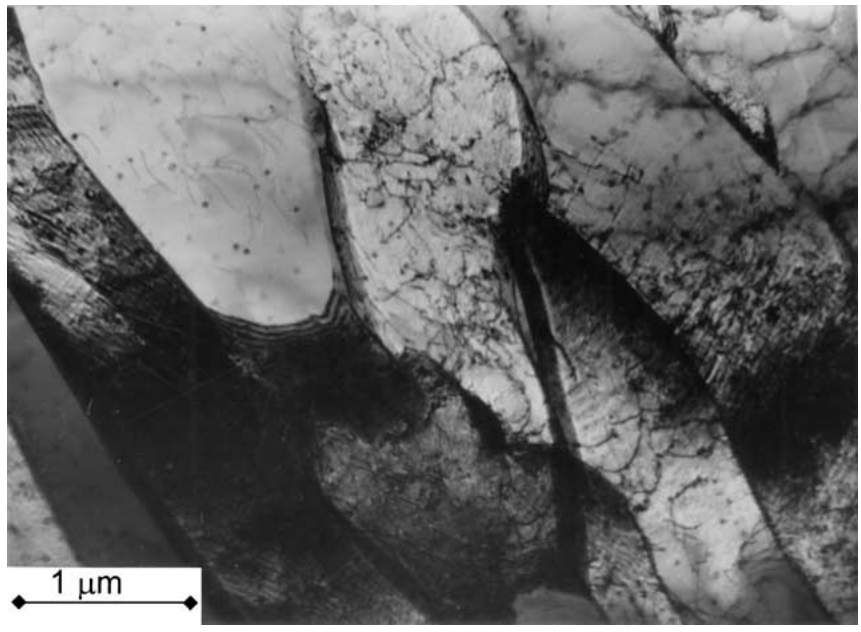

(a)

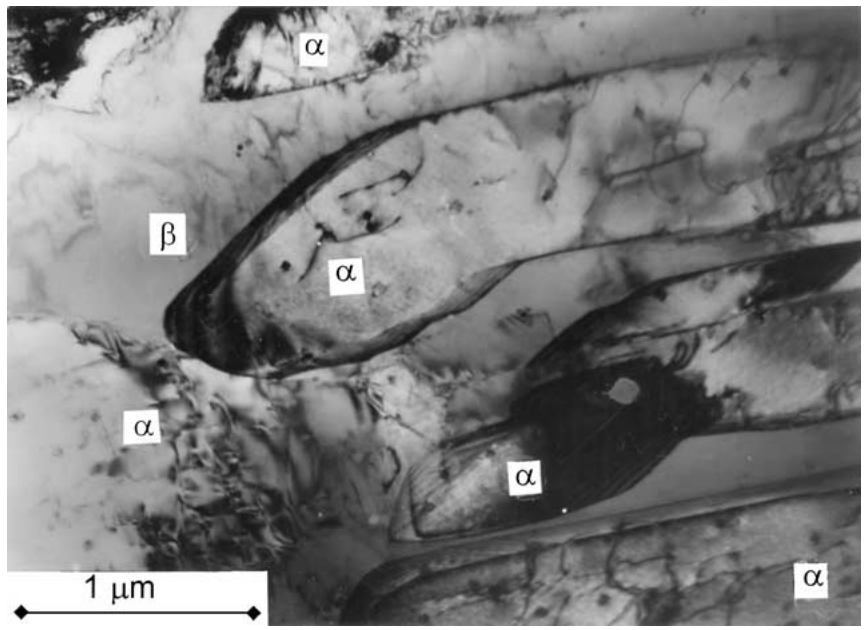

(b)

Figure 4 Transmission electron microscopy micrograph for CuZn39Pb3 alloy deformed $\varepsilon_t = 0.4$ at strain rate of 0.0007 s^{-1} and 1093 K: (a) highly recovered substructure within α-grain; (b) area of α and β phase (diffraction patterns were analyzed for subgrains marked in the Figure).

specific particle distribution mentioned above resulted most probably from higher solubility of iron at high temperature within β than within the α-matrix. Moreover, it seems reasonable that Fe-particle nucleation within α-phase during cooling was faster than that for β-grains.

Lead addition to Cu-Zn alloys is used practically in order to improve the machining properties of the material. Small Pb-particles may also reduce the final grain size due to retardation of the grain boundary migration (recrystallization fronts) during heat treatment or hot deformation of the material. An example of a typical particle in a hot deformed sample was shown in Fig. 5a. Most of the observed lead particles were close to spherical in shape. Lead particles were practically insoluble in the matrix and their coarsening during heat treatment was very limited. During hot deformation above the melting temperature of lead, lead inclusions, surrounded by solid matrix, did not practically affect the hardening of the material. It seems reasonable to conclude that it is the lead addition, which improves the mechanical properties of the material by pinning grain boundaries and retardation of grain growth, rather than the precipitation hardening of the alloy.

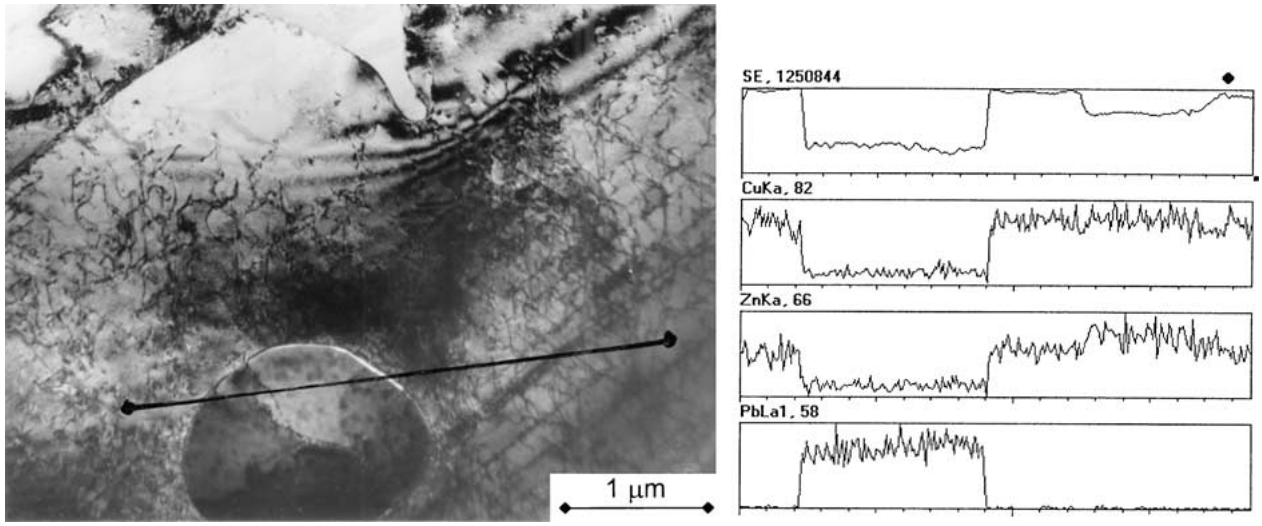

(a)

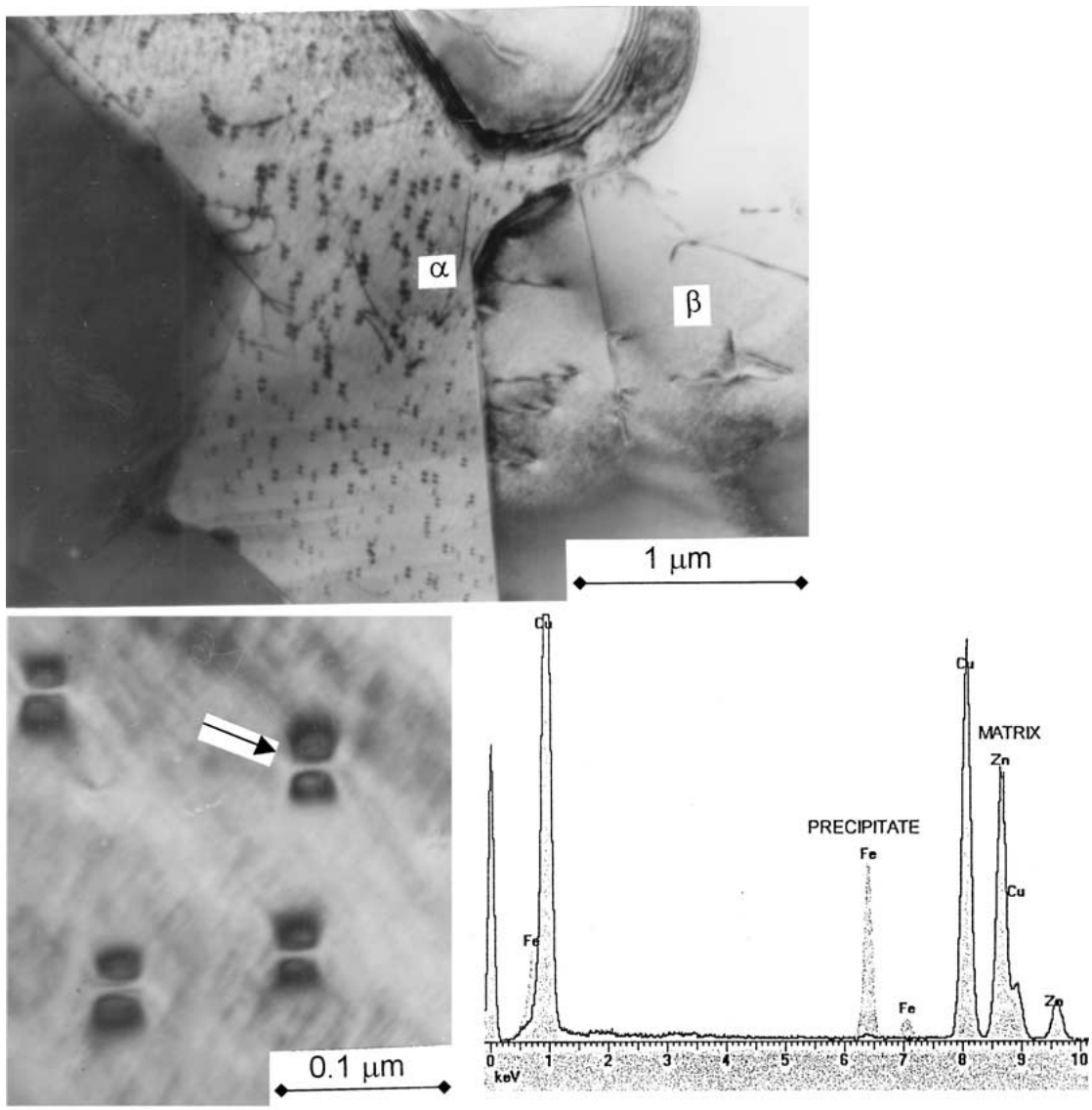

(b)

Figure 5 Structure of CuZn39Pb3 alloy annealed 3 min/1143 K and water quenched: (a) lead inclusion and X-ray line analysis taken from the particle and the neighboring matrix; (b) coherent precipitates of iron within α-grain. XEDS spectrum was taken from the particle marked in the enlarged part of α-grain.

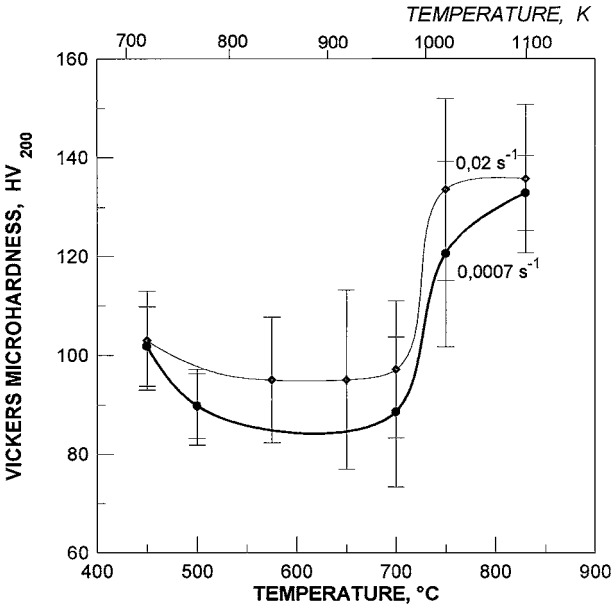

Figure 6 Vickers hardness vs. deformation temperature for samples deformed $\varepsilon_t \approx 0.4$ at strain rate of 0.02 s^{-1} and 0.0007 s^{-1}.

4. Conclusions

1. Reduction of the flow stress during hot deformation of CuZn39Pb3 alloy resulted from dynamic recovery and dynamic recrystallization which had operated above ~950 K. Fine lead particles did not fully protect the grain coarsening in the curse of dynamic recrystallization at high deformation temperatures. During hot deformation above ~1000 K, $\alpha \rightarrow \beta$ phase transformation was found overlapping the mentioned structural softening process and it resulted in effective grain coarsening. In result, effective flow stress reduction was observed.

2. The hardness of hot deformed alloy was reduced with increasing deformation temperature within the temperature range of 700 K–950 K. An increase of the material hardness was observed for samples deformed above ~950 K. The hardening effect was ascribed to grain refining which resulted from partial $\alpha \rightarrow \beta$ transformation and fine α/β structure development in result of water quenching after hot deformation.

3. Coherent Fe-particles were observed within some α-grains of water quenched samples deformed at 1093 K. Neighboring β-grains were free of Fe-precipitates. Specific distribution of Fe-precipitates was ascribed to higher solubility of iron in β than in α-matrix at high deformation temperature. In result, $\beta \rightarrow \alpha$ transformation during cooling resulted in local growth of α-grains of solution oversaturated with Fe. In result, precipitation of coherent Fe-particles created an additional hardening component competitive to the commonly accepted strain hardening and structural hardening due to the grain refining mentioned above.

Acknowledgements

The authors are grateful for financial support from the Polish Committee for Scientific Research (KBN) under grant No PB 501/T08/97/12. Foundation for Polish Science is acknowledged for the purchase of JEOL 2010 electron microscope.

References

1. J. J. JONAS, C. M. SELLARS and W. J. McG. TEGART, *Met. Rev.* **14** (1969) 1.
2. I. WEISS and J. J. JONAS, *Met. Trans.* **10A** (1979) 831.
3. A. KORBEL, L. BLAZ, H. DYBIEC, J. GRYZIECKI and J. ZASADZINSKI, *Metals Technology* **6** (1979) 391.
4. L. BLAZ and A. KORBEL, *Archiwum Hutnictwa* **27** (1982) 285 (in polish).
5. L. BLAZ, E. EVANGELISTA and M. NIEWCZAS, *Metallurgical and Materials Transactions* **25A** (1994) 257.
6. L. BLAZ, A. KORBEL and J. KUSINSKI, *Scripta Metallurgica et Materialia* **33** (1995) 657.
7. A. A. HAMEDA and L. BLAZ, *Materials Science and Engineering* **A254** (1998) 83.
8. L. BLAZ, in Proceedings of the XV Physical Metallurgy and Materials Science Conference on Advanced Materials and Technologies, AMT'98, Krakow-Krynica, Poland, May 1998, edited by J. Kusinski, I. Suliga and S. Kac, p. 447.
9. A. KORBEL and L. BLAZ, *Scripta Metall.* **14** (1980) 829.

Received 19 July 2000
and accepted 27 February 2001